Effect of Lead substitution On The Microstructural, Magnetic and Dielectric Properties of Barium Hexaferrite Powder

Reshma A. Nandotaria
Department of Physics
Gujarat University
Ahmedabad-380 009. India.
Cuteresh1979@yahoo.co.in
Rajshree B Jotania
Department of Physics
Gujarat University
Ahmedabad-380 009. India.
rbjotania@gmail.com

Chetna C. Chauhan
Institute of Technology
Nirma University
Ahmedabad 382 481, India.
chetna.chauhan@nirmauni.ac.in

***Abstract*—M-type hexaferrites with composition $Ba_{1-x}Pb_xFe_{12}O_{19}$ (x = 0.0 to 0.4) were prepared using a sol gel auto-combustion technique. The prepared as burnt powder samples were sintered at 950° C for 4 hours in a muffle furnace. The effect of lead substitution of barium hexaferrites on microstructural, magnetic and dielectric properties was investigated. The structural characterization on $Ba_{1-x}Pb_xFe_{12}O_{19}$ (x = 0.0 to 0.4) hexaferrite samples were carried out using X-ray diffraction (XRD) technique. The lattice parameters and cell volume of all samples were calculated. The X-ray diffraction patterns at room temperature reveal that the prepared samples have a single phase. Surface morphology and microstructural changes of prepared hexaferrite particles were examined using SEM and XRD. SEM images confirm the formation of hexagonal plate like particle and the addition of Pb increases the formation of plate like structures. The magnetic properties of prepared hexaferrite samples were investigated by using VSM and the dielectric measurements were carried out at room temperature in frequency ranges from 100 Hz to 2MHz.**

Keywords- Lead substitution; Ba-M hexaferrites; XRD; SEM;

I. INTRODUCTION

M-type hexaferrite $BaFe_{12}O_{19}$ (Ba-M) possesses magnetoplumbite structure and is one of the most widely used hard magnetic material in many applications like permanent magnet and microwave devices because of their high Curie temperature, high coercivity and high magnetocystalline anisotropy constant, high corrosion resistance, and excellent chemical stability [1,2].

The basic structure of unit cell of Ba-M ferrite is built by ten layers of oxygen ions, which are formed by a close packing of cubic or hexagonal stacked layers alternately. The crystal structure of Ba-M ferrite is built up by RSR*S*blocks, where R* and S* represent a rotation of 180° around the hexagonal c-axis.The S-block contains two oxygen layers forming a spinel block, whereas R block is a three layer block containing the layer with Ba ion. The Fe^{+3} ions occupy five different interstitial sites (12k, 2a, $4f_2$, $4f_1$, 2b) within the basic structure: three sites 12k, 2a and $4f_2$ configured positive to the magnetic (spin up) polarization and have an octahedral co-ordination, one site $4f_1$ has tetrahedral co-ordination, 2b has five fold co-ordination and both have negative (spin down) polarization. Several researches have been made attempt to modify its magnetic properties by substituting nonmagnetic ions in this materials that disturbs the magnetic moment of Fe^{+3} ions in the basic block. Magnetic properties of Co-Ti and Ru-Ti substituted barium ferrite nanocrystalline particles $Ba_{1-x}Fe_{12-2x}Co_xTi_xO_{19}$ with ($0 < x < 1$) and $Ba_{1-x}Fe_{12-2x}Ru_xTi_xO_{19}$ with ($0 < x < 0.6$) were studied by Alsmadi et al. [3]. Electrical and dielectric properties of M-type strontium hexaferrites doped with Gd-ions investigated by Katoch et al. [4]. Dielectric properties of cobalt substituted M-type barium hexaferrite prepared by co-precipitation studied by Shepherd et al. [5], while structural and magnetic properties of modified M-type $Ba_{1-x}Fe_{12-2x}Co_xSn_xO_{19}$ hexaferrites were studied by Soloveva et al. [6]. Y. Tokunaga et al. studied Magnetic and magnetoelectric (ME) properties of Sc-doped M-type barium hexaferrites [7]. A strong magneto-optical activity in rare-earth La^{3+} substituted M-type strontium ferrites by Hu et al. [8].Very less attempt has been made on study of magnetic, dielectric and structural properties of lead substituted barium hexaferrite.

Many synthesis methods have been proposed for the preparation of Ba-M hexaferrite like ceramic [9], chemical co-precipitation route [10], sol-gel [11], low temperature auto combustion [12], micro emulsion and reverse microemulsion [13] etc. Literature survey reveals that the substitution of Pb in R block perturbs the S block in the crystal structure, which must be responsible for the formation of impurity phase [14,15]. Lead doped materials have become more attractive because of their low anisotropic field and fast crystallization

process. A sol gel auto combustion method was used to control the impurity phase at low temperatures.

In the present paper, we report the structural, magnetic and dielectric properties of Pb doped barium hexaferrites.

II. EXPERIMENTAL

A. *Materials and Methods*

Ferric Nitrate [($Fe(NO_3)_3$) 98% Purity, Sigma Aldrihic], Barium nitrate [$Ba(No_3)_2$ 98% Purity, Merck], Lead nitrate [$Pb(No_3)_2$], citric acid [$C_6H_8O_7$] and Ammonia solution were used as raw materials to prepare $Ba_{1-x}Pb_xFe_{12}O_{19}$ (x = 0.0, 0.1, 0.2, 0.3, and 0.4) hexaferrite samples.

B. *Synthesis*

Stochiometric amount of barium nitrate, ferric nitrate and lead nitrate were dissolved one by one in deionised water followed by the addition of citric acid solution. An ammonia solution was added to adjust the pH value 7.0.The mixed solution was slowly evaporated in air at 80 °C until the viscous gel was obtained. It was dried at 110°C and turned into dried gel. The dried gel was ignited in air and finally was sintered at 950°C for 4 hours in a muffle furnace to prepare $Ba_{1-x}Pb_xFe_{12}O_{19}$ (x = 0.0, 0.1, 0.2, 0.3, and 0.4) hexaferrite powder samples. Prepared samples cheresterized using various experimental techniques like XRD, SEM, VSM and dielectric measurements.

C. *Characterization*

A Bruker D Z Phaser diffractometer (PW 1830) was used to obtain X-ray powder diffraction (XRD) pattern (Cu- Kα radiation (λ=1.5405 Å) with a step scan 0.02ºC/min) and to determine the crystal structure of prepared hexaferrite powder. The scanning electron micrographs were taken on a Make-Leo/Lica model Stereo scan 440 scanning electron microscope (SEM) in order to observe the particle size and morphology. The hysteresis loop of the hexaferrite powder samples was recorded at room temperature using a vibrating sample magnetometer (VSM). The dielectric measurements were carried out using LCR meter *(*Hewlett Packard *4284A*) at room temperature in the frequency range from 100 Hz to 2 MHz.

III. RESULTS AND DISCUSSION

A. *Crystal Structure*

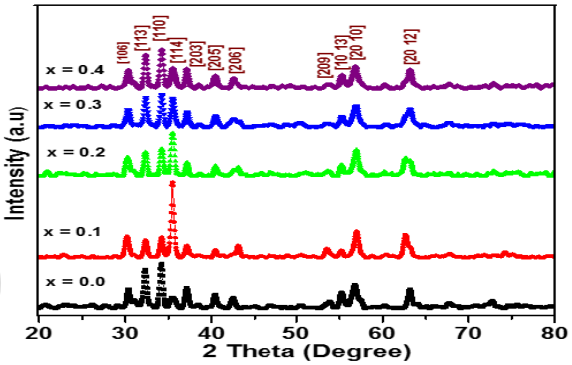

Figure 1. X-ray diffraction patterns of $Ba_{1-x}Pb_xFe_{12}O_{19}$ (x = 0.0, 0.1, 0.2, 0.3, and 0.4) samples calcinated at 950ºC.

TABLE I. LATTICE CONSTANT a, c AND VOLUME OF UNIT CELL (V) AND X-RAY DENSITY FOR $Ba_{1-x}Pb_xFe_{12}O_{19}$

Pb concentration x	Lattice Parameter a (Å)	Lattice Parameter c (Å)	c/a	Cell Volume V(Å)^3
0.0	5.235	23.195	4.430	550.49
0.1	5.359	23.290	4.346	579.24
0.2	5.589	23.895	4.275	646.39
0.3	5.895	23.600	4.003	710.23
0.4	5.589	23.895	4.275	646.39

TABLE II. PARTICLE SIZE FROM FROM DEBYE SCHERRER FORMULA

Pb concentration x	Theta (degree)	d-spacing Observed [Å]	Cos θ	Crystalline size D [nm]
0.0	17.745	2.527	0.952	10.064
0.1	17.749	2.526	0.952	21.644
0.2	17.749	2.527	0.952	17.231
0.3	17.755	2.525	0.952	15.814
0.4	17.744	2.527	0.952	13.575

The powder X-ray diffraction pattern of $Ba_{1-x}Pb_xFe_{12}O_{19}$ samples with x = 0.0, 0.1, 0.2, 0.3 and 0.4 are shown in figure 1. In all the samples M-type hexaferrite appears as a major

phase; which indicates that Fe^{+3} ions are substituted by the Pb^{+2} ion in the crystallographic structure of $Ba_{1-x}Pb_xFe_{12}O_{19}$. The lattice parameters ***a*** and ***c*** were calculated from the values of d_{hkl} corresponding to [114] peak (Table 1). The calculated lattice parameters are in close agreement with the standard JCPDS file- PDF# 840757. Lattice parameters of $Ba_{1-x}Pb_xFe_{12}O_{19}$ for x = 0.0, 0.1 samples are slightly smaller than that of $BaFe_{12}O_{19}$ [16]. This slight change in the lattice parameter may be due to the difference between the ionic radius of Pb^{+2} and Fe^{+3} (0.645 Å).The lattice parameters are observed to be increasing with increasing Pb-content (x= 0.2) and then it decreases due to the difference in ionic radius. Lattice volume of all the samples were calculated using the equation

$$V = \frac{3}{\sqrt{2}} a^2 c \qquad (1)$$

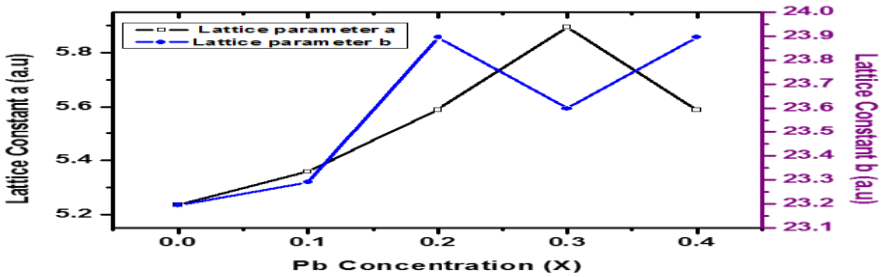

Figure 2. Variation of lattice parameters with lead concentration

The average crystalline size of hexaferrite powder was calculated by the X-ray line broadening technique using Debye Scherrer formula [17] using the profile of (1 1 4) peak as shown in table 2.

$$d = 0.9\frac{\lambda}{\beta \cos\theta} \qquad (2)$$

where λ is the X-ray wavelength, θ is the angle of Bragg diffraction and β is the difference between FWHM and the instrumental broadening.

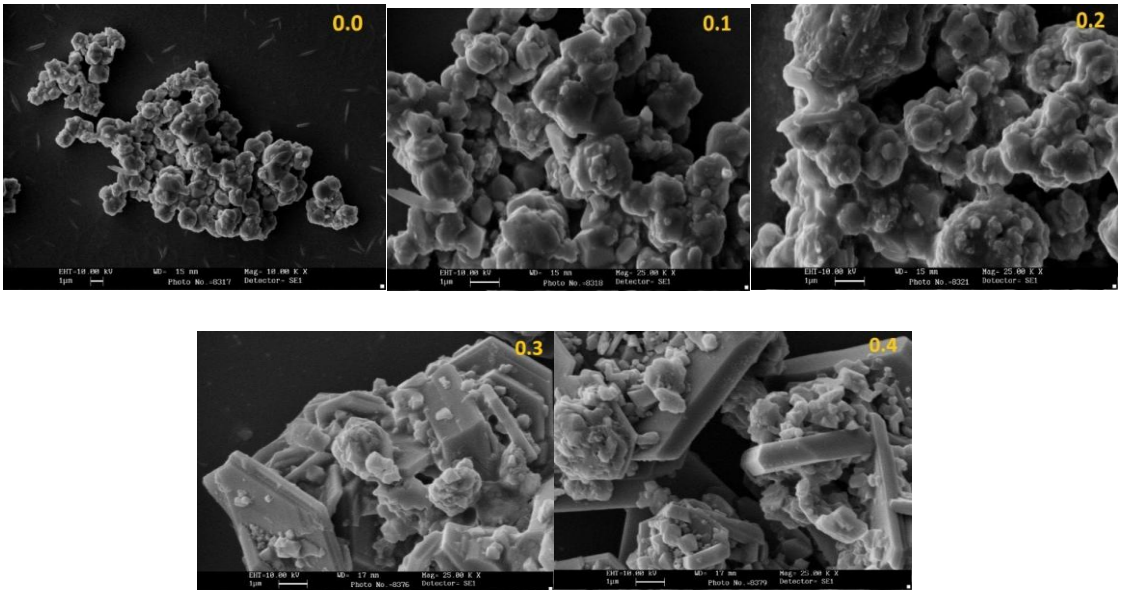

Figure 3. SEM micrographs of $Ba_{1-x}Pb_xFe_{12}O_{19}$ (x = 0.0, 0.1, 0.2, 0.3, and 0.4) samples calcinated at 950ºC.

B. Morphology

The microstructure and surface morphology of $Ba_{1-x}Pb_xFe_{12}O_{19}$ (x = 0.0 to 4.0) particles were observed by scanning electron microscope (SEM) technique and the images are shown in figure 3.The pure barium hexaferrite is observed the agglomeration of the particles. Sharp and well defined edges of plate like structures are developed with the increase in the lead concentration [18].

C. Magnetic Properties

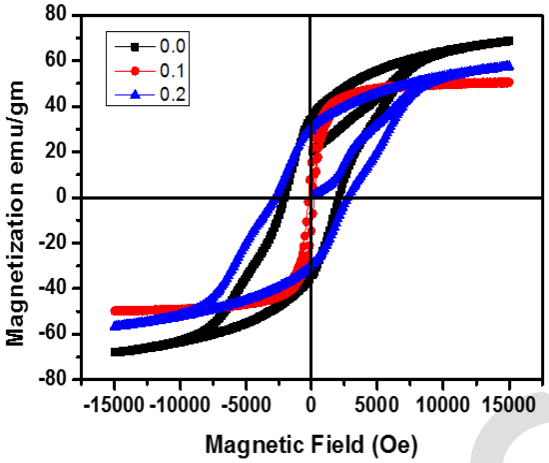

Figure 4. Magnetic hysteresis loops for $Ba_{1-x}Pb_xFe_{12}O_{19}$ (x = 0.0, 0.1 and 0.2) samples calcinated at 950ºC.

Figure 4 shows the field dependent magnetization of $Ba_{1-x}Pb_xFe_{12}O_{19}$ (x=0.0, 0.1 and 0.2) samples measured at room temperature in an applied field of 15kOe.Saturation Magnetization(Ms), Coercivity (Hc), retaintivity (Mr) and squareness ratio (Mr/Ms) have been calculated from hysteresis loops. The hysteresis loops displays the characteristics of the hard magnetic materials. The magnetization increases with the increase in an external magnetic field strength at low field region and attains a maximum value for the field ~15kOe.Table 3 show that Pb doping has changed the axis length and c axis length, which resulted in the formation of hexagonal plate like structures. There is change in the morphology and amount of grain boundaries in each Pb^{+2} ions substitutions. Magnetocrystalline anisotropy constant is an important parameter to explain the variation of magnetic properties. The decrease in coercivity is due to the interruption in domain wall motion and increase in grain size. As shown in table 3 the saturation magnetization decreases with the increase in Pb content [19]. With increase in non magnetic lead ion results in super exchange interaction of Fe^{+3} ions in two sublattices of have opposite spin. dopant possess the volatile nature and are in R block, they cause the super exchange to have spin in phase and as a result of which saturation magnetization decreases.

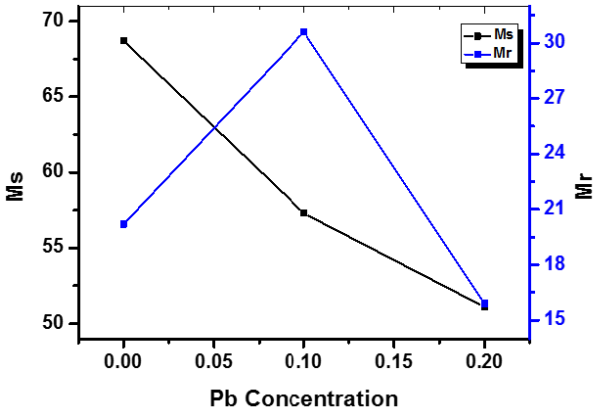

Figure 5. Variation of Mr and Ms for $Ba_{1-x}Pb_xFe_{12}O_{19}$ (x = 0.0, 0.1 and 0.2) samples calcinated at 950ºC.

TABLE III ESTIMATION OF MAGNETIC PARAMETERS OF Pb DOPED HEXAFERRITE

Pb content (x)	M_s (emu/g)	M_r (emu/g)	M_r/M_s	H_c(Oe)	K [HA^2/Kg]
0.0	68.7	20.2	0.294	4020	0.173×10^{-3}
0.1	57.3	30.6	0.533	522	0.187×10^{-4}
0.2	51.1	15.9	0.311	5301	0.170×10^{-4}

D. *Dielectric Properties*

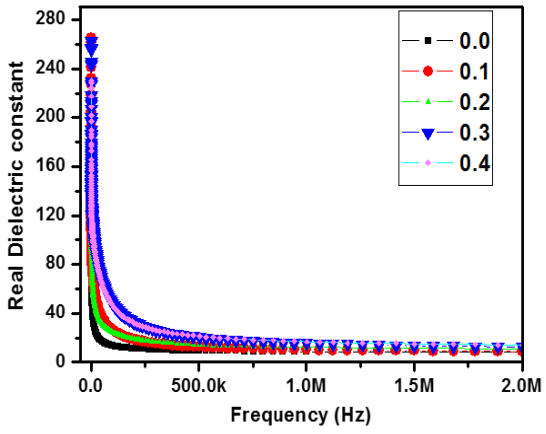

Figure 6. Variation of Real dielectric constant with frequency for $Ba_{1-x}Pb_xFe_{12}O_{19}$ (x = 0.0, 0.1 0.2,0.3 and 0.4) samples calcinated at 950ºC.

Figure 6 shows the variation of real dielectric constant with frequency at room temperature in the frequency range 100Hz to 2 MHz. The dielectric constant decreases continuously with increase in frequency. This dielectric dispersion in ferrites can be explained on the basis of

interfacial polarization given by Maxwell-Wagner model. The dielectric structures of ferrite consists of conducting grains that are separated by the grain boundaries that are poor conductors. The grain boundaries and produce polarization. As the frequency of the externally applied electric field is increased, the electrons hopping between Fe^{+2} and Fe^{+3}does not follow the externally applied electric field as a result dielectric constant decreases and then it becomes constant.At lower frequencies the dispersion of dielectric constant is low as compared to that of the higher frequencies (~100 KHz) after which it reaches a constant value.

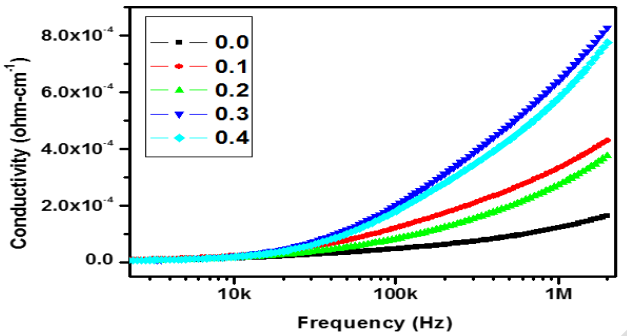

Figure 7. Variation of ac conductivity with frequency for $Ba_{1-x}Pb_xFe_{12}O_{19}$ (x = 0.0, 0.1 ,0.2, 0.3 and 0.4) samples calcinated at 950ºC.

Figure 7 shows the variation of ac conductivity with temperature.As the applied frequency competes with the jump frequency the conductivity remains constant first at lower frequencies and then after it increases with the increase in frequency.Electron hopping and defect dipoles are responsible for the origin of dielectric loss in ferrites. The electron hopping contributes to the dielectric loss only in lower frequency range.

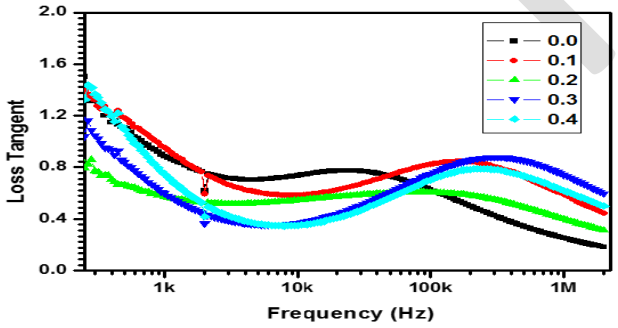

Figure 8. Variation of of dielectric loss tangent with frequency for $Ba_{1-x}Pb_xFe_{12}O_{19}$ (x = 0.0, 0.1 ,0.2, 0.3 and 0.4) samples calcinated at 950ºC.

The response of electron hopping is decreased with the increase in frequency and hence the dielectric loss decreases in the higher frequency range as shown in figure 8.When the hopping frequency of the electron between Fe^{+2} and Fe^{+3} ions is close to the frequency of the external applied field the dielectric loss peaks are observed as shown in figure 8.The loss peak is moving to high frequency side with the increase in Pb content. This may be due to the fact that lead substitution prefers the octahedral site which in turn strengthens the dipole-dipole interaction that restricts the rotation of the dipoles.

IV SUMMARY

In the summary it may be concluded that a series of Ba-M ferrite with compositional formula Ba_{1-x} $Pb_xFe_{12}O_{19}$ where x = 0.0, 0.1, 0.2, 0.3 and 0.4 were prepared by a sol gel auto combustion technique. The structural, magnetic and dielectric properties investigated. The crystalline size of prepared samples are found to increases with the increase in the lead content. Plate like particles with sharp edges is observed for the higher Pb content. The saturation magnetization decreases with increase of Pb substitution. The frequency dependence dielectric loss tangent shows the abnormal behaviour of loss peak due to the dipole -dipole interaction. The synthesized hexaferrite is very useful for magnetic recording media and data storage devices.

V ACKNOWLEDGEMENT

One of the authors (Reshma A. Nandotaria) gratefully acknowledges financial support of this work in the form of Rajiv Gandhi National Fellowship New Delhi, India. This work is supported by DRS-SAP program of UGC, New Delhi, India.

VI REFERENCES

[1] N. Shams, X. Liu,M. Matsumoto, A. Morisake, J. Magn. Magn. Mater, vol. 290, pp. pp.138-140, 2005.
[2] O.Carp, R.Barjega, E. Srgal, M. Brezeanu, Thermochemica Acta vol. 318, pp.57-62, 1998.
[3] A. M. Alsmadi, I. Bsoul, S. H. Mahmood, G. Alnawashi, K. Prokeš, K. Siemensmeyer, B. Klemke and H. Nakotte J. Appl. Phys., vol. 114, pp. 243910, 2013.
[4] Arun Katoch, B. K. Borthakur, Anterpreet Singh, Taminder Singh, Int J. of Engineering Research & Technology, vol. 2 (3), 2013.
[5] Philip Shepherd Æ Kajal K. Mallick Æ Roger J. Green, J Mater Sci: Mater Electron, vol. 18, pp.527–534, 2007.
[6] E. D. Solov'eva, E. V. Pashkova, A. E. Perekos, A. G. Belous, Ino Mater, vol. 48 (11), pp1147-1152, 2012.
[7] Y. Tokunaga, Y. Kaneko, D. Okuyama, S. Ishiwata, T.Arima, S.Wakimoto, K.Kakurai, Y. Taguchi, and Y. Tokura, Phys. Rev. Lett., vol. 105, pp.25720, 2010.
[8] Feng Hu, Lucia Fernandez-Garcia, Xian-Song Liu, De-Ru Zhu, Marta Suárez et al.: J. Appl. Phys., vol. 109, pp.113906, 2011.
[9] Y. Liu, M.G.B. Drew, Y. Liu, J. Magn. Magn. Mater., vol. 323,pp.945–953, 2011.
[10] R. C. Pullar, Progress in Materials Science, vol. 57, pp. 1191-1334 2012..
[11] M. Manjural Haque, M. Heq,M. A. Hakim, Mater. Chem. Phys., vol. 112, pp.580-586, 2008.
[12] A. Haq,M. Anis-ur-Rehman, Physica B, vol. 407,pp.822–826, 2012.
[13] Y. Liu,M.G.B. Drew,Y. Liu, J. Magn. Magn. Mater., 323 (2011),pp. 945–953.
[14] S.G. Kim, W.N. Wang,T. Iwaki, J. Phys. Chem. C, vol. 111, pp. 10175–10180 2007.
[15] J. C. Maxwell, Oxford University Press, New York, vol. 1, pp. 828, 1973.
[16] K. W. Wagner, Annalen der Physik, vol. 40, pp. 817-855 1913.
[17] M. A. Ahamad, J. Elhiti, Physique III, vol. 5, pp. 775, 1995.
[18] M. Snaikh, S. S. Bellard,B. K. Chougule, J. Magn. Magn. Mater, vol. 195, pp. 384-390, 1999.
[19] M. A. Ahamad, J. Elhiti, E. I. Nimar, A. M. Amar, J. Magn. Magn. Mater., vol. 152, pp.391-395, 1996.